THE JOURNAL OF BIOLOGICAL CHEMISTRY VOL. 289, NO. 40, pp. 28040–28053, October 3, 2014

Vesicle Associated Membrane Protein 8 (VAMP8)-mediated Zymogen Granule Exocytosis Is Dependent on Endosomal Trafficking via the Constitutive-Like Secretory Pathway*

Received for publication, July 2, 2014, and in revised form, August 11, 2014 Published, JBC Papers in Press, August 19, 2014, DOI 10.1074/jbc.M114.593913

Scott W Messenger[‡1], **Michelle A. Falkowski**[‡1], **Diana D. H. Thomas**[‡], **Elaina K. Jones**[‡], **Wanjin Hong**[§], **Herbert Y. Giasano**[¶], **Nicholas M. Boulis**[‖], **and Guy E. Groblewski**[‡2]

From the [‡]*Department of Nutritional Sciences, University of Wisconsin, Madison, Wisconsin 53706,* [§]*Institute of Molecular and Cellular Biology, National University of Singapore, Singapore 138673,* [¶]*Departments of Medicine and Physiology, University of Toronto, Ontario M5S 1A8, Canada, and* [‖]*Department of Neurosurgery, Georgia Institute of Technology, Atlanta, Georgia 30322*

Background: Acinar cells contain two vesicle-associated membrane proteins (VAMP) 2 and 8 for secretion.
Results: WT and VAMP8 knock-out acini expressing various regulatory protein constructs demonstrate VAMP2 regulates early and VAMP8 late phases of secretion.
Conclusion: VAMP8- but not VAMP2-mediated secretion is dependent on anterograde endosomal trafficking.
Significance: Results provide mechanistic insight into how different zymogen granule VAMPs shape secretion.

Acinar cell zymogen granules (ZG) express 2 isoforms of the vesicle-associated membrane protein family (VAMP2 and -8) thought to regulate exocytosis. Expression of tetanus toxin to cleave VAMP2 in VAMP8 knock-out (−/−) acini confirmed that VAMP2 and -8 are the primary VAMPs for regulated exocytosis, each contributing ~50% of the response. Analysis of VAMP8$^{-/-}$ acini indicated that although stimulated secretion was significantly reduced, a compensatory increase in constitutive secretion maintained total secretion equivalent to wild type (WT). Using a perifusion system to follow secretion over time revealed VAMP2 mediates an early rapid phase peaking and falling within 2–3 min, whereas VAMP8 controls a second prolonged phase that peaks at 4 min and slowly declines over 20 min to support the protracted secretory response. VAMP8$^{-/-}$ acini show increased expression of the endosomal proteins Ti-VAMP7 (2-fold) and Rab11a (4-fold) and their redistribution from endosomes to ZGs. Expression of GDP-trapped Rab11a-S25N inhibited secretion exclusively from the VAMP8 but not the VAMP2 pathway. VAMP8$^{-/-}$ acini also showed a >90% decrease in the early endosomal proteins Rab5/D52/EEA1, which control anterograde trafficking in the constitutive-like secretory pathway. In WT acini, short term (14–16 h) culture also results in a >90% decrease in Rab5/D52/EEA1 and a complete loss of the VAMP8 pathway, whereas VAMP2-secretion remains intact. Remarkably, rescue of Rab5/D52/EEA1 expression restored the VAMP8 pathway. Expressed D52 shows extensive colocalization with Rab11a and VAMP8 and partially copurifies with ZG fractions. These results indicate that robust trafficking within the constitutive-like secretory pathway is required for VAMP8- but not VAMP2-mediated ZG exocytosis.

Pancreatic acinar cells undergo robust constitutive and regulated secretion of large quantities of digestive enzymes necessary for nutrient digestion and are a classic model to study polarized epithelial protein secretion (1). Digestive enzymes or zymogens are condensed in the *trans*-Golgi and emerge in the cytoplasm as large immature secretory granules that then undergo a poorly defined maturation process resulting in the formation of large (~1-μm diameter) zymogen secretory granules (ZGs).[3] The ZGs accumulate as a storage pool that undergoes exocytosis over the next 2–24 h in response to hormone/neurotransmitter stimulation of G-protein-coupled receptors. As is well accepted in all cells, exocytosis is mediated by SNARE complex assembly composed of vesicle-associated membrane protein (VAMP) or vSNAREs on ZGs that interact with plasma membrane (PM) target or tSNAREs of the syntaxin and SNAP25 families (2). Previous studies have implicated a number of tSNAREs in acinar exocytosis including SNAP23 (on PM and ZGs), syntaxin 2 (apical PM), syntaxin 3 (on ZGs) and syntaxin 4 (on basolateral and apical PM) (for review, see Ref. 3). Two vSNAREs have also been identified on ZGs; VAMP2, a major secretory vesicle SNARE involved in neural and endocrine secretion, and VAMP8, a ubiquitous SNARE originally identified as playing a role in endosomal vesicle fusion.

One of the first demonstrations of a SNARE protein to regulate exocytosis outside of the nervous system was identified by introducing tetanus toxin (TeTx) into streptolysin-O-permeabilized acinar cells to selectively cleave VAMP2, resulting in an ~30% reduction of Ca^{2+}-stimulated amylase secretion (4). This

* This work was supported, in whole or in part, by National Institutes of Health Grant DK07088 (to G. E. G.). This work was also supported by United States Department of Agriculture/HATCH Grant WIS01583 (to G. E. G.).
[1] Both authors contributed equally to this work.
[2] To whom correspondence should be addressed: Dept. of Nutritional Sciences, 1415 Linden Dr., Madison, WI 53706; Tel.: 608-262-0084; Fax: 608-262-5860; E-mail: groby@nutrisci.wisc.edu.

[3] The abbreviations used are: ZG, zymogen granule; VAMP, vesicle-associated membrane protein; VAMP8$^{-/-}$, VAMP8 knockout; TeTx, tetanus toxin; Ti-VAMP7, tetanus toxin-insensitive VAMP7; CLP, constitutive-like secretory pathway; MRP, minor regulated pathway; PM, plasma membrane; EE, early endosome; LE late endosome; RE, recycling endosome; EEA1, early endosomal antigen 1; CCK-8, cholecystokinin-8; syt1, synaptotagmin 1; TG, thapsigargin; TPA, 12-*O*-tetradecanoylphorbol-13-acetate; CPT-cAMP, 8-(4-chlorophenylthio)adenosine 3′,5′-cyclic monophosphate; vSNARE, vesicle SNARE; tSNARE, target SNARE; LAMP1, lysosome-associated membrane protein 1.

was later confirmed by introducing additional proteins into permeabilized acini including 1) soluble VAMP2 constructs to sequester membrane-attached SNAREs, 2) neutralizing antibodies to VAMP2, or 3) botulinum neurotoxin B, also known to cleave VAMP2, each of which showed an ~40–50% reduction in Ca^{2+}-stimulated secretion (5–7). The lack of complete inhibition indicated that additional VAMP isoforms likely play a role in ZG exocytosis. The first evidence for VAMP8 as a ZG vSNARE was unexpectedly discovered in VAMP8 knock-out mice (VAMP8$^{-/-}$), which showed gross morphological abnormalities in exocrine tissues of pancreas, parotid, and lacrimal glands (8, 9). Isolated VAMP8$^{-/-}$ acini were reported to undergo a >50% reduction in amylase secretion when calculated as a percent of total cellular amylase (10).

Despite the large diameter of ZGs, acinar cells have a limited apical PM, comprising only ~5% of total cell surface area. This was proposed to be mitigated by the process of sequential compound exocytosis (PM-ZG-ZG fusion) (11, 12). Live cell imaging studies in isolated acini have shown that ZGs remain fused with the apical PM for several minutes, allowing for the fusion of one or more ZGs to the primary granule (11, 13, 14). We previously provided evidence that acinar cells have at least two populations of ZGs based on their relative expression of VAMP2 and VAMP8 (6). VAMP2 accumulates in the most apical regions along the PM and within cortical actin web under basal conditions, whereas VAMP8 is recruited more slowly to the apical PM with cell stimulation (6). In the current model for compound sequential ZG exocytosis, VAMP2-positive ZGs were proposed to initially fuse with the PM and contain the requisite tSNAREs, syntaxin 3 and SNAP23, to interact with VAMP8, thereby promoting ZG-ZG fusion (10, 15). Supporting this, acini from VAMP8$^{-/-}$ mice are deficient in compound exocytosis, potentially explaining the reduced secretion found in these animals (10). However, intravital two-photon microscopy of the parotid gland conducted at 37 °C in live animals identified that ZGs completely fuse with the PM, and their membrane is retrieved in less than 1 min to prevent significant expansion of the PM. Subsequent ZGs fuse directly with the PM, and compound ZG fusion is not observed (16).

In addition to the classic ZG pathway, two parallel secretory pathways were previously described based on the rapid secretion of pulse-labeled zymogens from isolated pancreatic and parotid lobules; these were termed the constitutive-like (CLP) and minor-regulated pathways (MRP) (17–19). The CLP/MPR were proposed to provide small amounts of secretion during the interdigestive period and to potentially deliver tSNAREs to the plasma membrane necessary for ZG exocytosis. The CLP and MRP were proposed to originate by clathrin-dependent budding from the *trans*-Golgi and immature secretory granules and undergo anterograde trafficking through endosomal intermediates before fusing with apical PM (20–22). We recently reported that when placed in culture (16 h), acinar cells lose ~50% of their stimulated-secretory response with no apparent decrease in the expression of SNAREs necessary for ZG exocytosis. Rather, cultured acini experience a rapid loss of the early endosomal regulatory protein Rab5 and its interacting proteins tumor protein D52 (D52) and early endosomal antigen 1 (EEA1) (23, 24). Restoration of D52 by adenoviral expression coinduces the expression of Rab5 and EEA1 and restores a majority of the secretory response. Furthermore, expressed D52 was found to strongly colocalize with Rab11a, a primary component of the apical recycling endosomal (RE) compartment. Use of the Golgi- and endosomal-disrupting agent brefeldin A together with cell surface labeling of the endolysosomal protein, lysosome-associated membrane protein 1 (LAMP1), implicated Rab5/D52/EEA1-mediated endosomal trafficking in regulating the secretory activity of the CLP/MRP (22). Results that a complete loss of the CLP/MRP compromised only half of the secretory response raised an important question regarding whether 1) the CLP/MRP are only indirectly involved in ZG exocytosis or 2) acinar cells have two pathways mediating ZG exocytosis, one of which is directly regulated by the CLP/MRP.

VAMP8 was originally named endobrevin as it localizes to early (EE) and late (LE) endosomes in most cells and was shown to play a functional role in homotypic endosomal fusion *in vitro* (25). In addition to its presence on ZGs, VAMP8 has been shown to regulate secretory granule exocytosis in cytotoxic T lymphocytes, mast cells, platelets, goblet cells, and pancreatic β-cells (26–30). In most of these cell types VAMP8-containing secretory granules retain various amounts of membrane and cargo proteins characteristic of endosomes and/or lysosomes potentially providing a clue to the relationship of the endosomal/lysosomal compartment to VAMP8-containing secretory granule formation/maturation. In the current study we investigated the nature of VAMP2- *versus* VAMP8-mediated secretion by utilizing acinar cells from WT and VAMP8$^{-/-}$ mice together with short term (4 h) adenoviral expression of TeTx light chain, which selectively cleaves VAMP2 on ZGs. We further examined how altering endosomal trafficking acutely alters ZG exocytosis mediated by these SNAREs. Results support that VAMP2-mediated exocytosis controls an early rapid phase of secretion likely mediated by synaptotagmin 1 (syt1), the Ca^{2+} sensor for exocytosis in nerve and endocrine cells (31). In comparison, VAMP8-mediated exocytosis produces a prolonged phase of secretion that requires an intact early endosomal compartment to function. Additional evidence is provided supporting that maturation of the VAMP8-positive ZG pathway requires robust trafficking within the CLP and involves the movement of the endosomal proteins D52 and Rab11a to the ZG compartment.

EXPERIMENTAL PROCEDURES

Antibodies—Antibodies against D52 (32) and CRHSP24 (33) were previously described. Antibodies for Rab11a (catalog no. ab78337), Rab5 (catalog no. ab18211), TI-VAMP7 (catalog no. ab36195), LAMP1 (catalog no. ab24107), VAMP8 (used for some immunofluorescence, catalog no. ab89158), and VAMP4 (ab3348) were from AbCam. Antibodies for VAMP2 (catalog no. 104211), VAMP8 (cat. no. 104303), and syntaxin 3 (catalog no. 110032) were from Synaptic Systems. Anti-EEA1 (catalog no. 610456) was from BD Biosciences. Antibodies for syt1 (catalog no. s2177) and VAMP2 (used for some immunofluorescence, catalog no. gw21451) were from Sigma. An antibody for Rab11a (used for some immunofluorescence, cat. no 71-5300) was from Invitrogen. A VAMP7 antibody (used for

some immunofluorescence, catalog no. SC32592) was from Santa Cruz. Anti-hemagglutinin mouse monoclonal antibody was purchased from Cell Signaling Technology. The antibody to pancreatic lipase was a kind gift from Mark Lowe (University of Pittsburgh) (34). Anti-Alexa-conjugated rabbit and mouse secondary antibodies were from Invitrogen. Peroxidase-conjugated secondary antibodies were from GE Healthcare. All antibodies were characterized before Western blotting and immunofluorescence labeling studies by serial dilutions to determine optimal conditions and negative controls (usually secondary antibody alone) to ensure specificity.

Other Reagents—Phadebas Amylase Assay kit was from Magle Life Sciences, cholecystokinin (CCK-8) was from Research Plus, Dulbecco's minimal essential medium (DMEM), essential amino acids, fetal bovine serum, TrypLE Express, penicillin and streptomycin, Alexa-conjugated phalloidin, and Image-iT® FX Signal Enhancer and Prolong gold antifade reagent with 4,6-diamidino-2-phenylindole (DAPI) were all from Invitrogen. Bovine serum albumin, 12-*O*-tetradecanoylphorbol-13-acetate (TPA), 8-(4-chlorophenylthio) adenosine 3′,5′-cyclic monophosphate (CPT-cAMP), and a protease inhibitor mixture containing 4-(2-aminoethyl)benzenesulfonyl fluoride, aprotinin, EDTA, leupeptin, and E64 were from Calbiochem. Protein determination reagent, Bio-Beads, and nonfat dry milk were from Bio-Rad. DNA Maxi, Mini-prep kits, PCR reagents, and CytoTox 96 were purchased from Promega. SuperSignal West Femto Chemiluminescent Substrate was from Thermo Scientific. All other reagents were purchased from Sigma. EGFP-Rab11a S25N adenovirus was a kind gift from Rejji Kuruvilla (Johns Hopkins University). HA-D52 and GFP adenovirus were previously described (22). TeTx adenovirus was previously described (35). Harvested adenovirus from AD-293 was purified and concentrated by cesium chloride centrifugation. Adenovirus titer was determined by plaque assay using agarose overlay on AD-293 cells.

Isolation and Short Term Culture of Pancreatic Acini—The University of Wisconsin Committee on Use and Care of Animals approved all studies involving animals. The previously generated VAMP8$^{-/-}$ mice from C57/BL6 background were genotyped with PCR, and VAMP8$^{-/-}$ animals were compared with WT litter mates (8). Pancreatic acini were isolated from male mice by collagenase digestion as previously described (36). Culturing of acini was performed similarly to the method described by Chen *et al.* (37). In brief, isolated acini were cultured in 100 × 15-mm plastic Petri dishes in 20 ml of DMEM supplemented with 0.5% FBS, 0.02% soybean trypsin inhibitor, penicillin, and streptomycin for the indicated times at 37 °C, 5% CO_2 in a humidified atmosphere. Adenoviruses were added to acini at specified titers in the culture medium for 4–16 h incubation. In control experiments >99% of acini expressed GFP when added at 10^5 pfu/ml for 16 h. Protein expression was optimized for each adenovirus by immunoblotting or in the case of TeTx measuring VAMP2 cleavage in cell lysates. Additionally cell viability for all experimental conditions was determined by measuring leakage of cytosolic lactate dehydrogenase to the medium over the final 3 h of culture (Table 1).

Acinar Secretory Assays—Pancreatic acini were stimulated as previously described, and amylase released to the medium was determined by Phadebas amylase assay as previously described (22, 36). Secretion was expressed as a percent of total cellular amylase and/or as amylase absorbance units normalized to total cellular DNA. DNA concentration was measured using the Hoechst reagent. Because cellular amylase activity and DNA concentration were determined to be directly proportional (r = 0.99), for some experiments DNA concentration was determined from total cellular amylase activity based on a standard curve. All data are the mean and S.E. of at least three separate tissue preparations performed in duplicate or triplicate. p values were calculated using a paired Student's t test.

TABLE 1

Lactate dehydrogenase activity present in the media was measured following 3 h incubation of acini and expressed as percent of total cellular Lactate dehydrogenase activity

As a positive control acini were stimulated with 10 nM CCK for 3 h to induce cell damage resulting in a 5 fold increase in LDH leakage. * < 0.05, n = 3 independent experiments each performed in duplicate.

Time	Sample	Treatment	LDH Release % of Total Cell LDH (mean +/- SE)
		Freshly Prepared Cells	
3 h	Wt	Basal	1.1 ± 0.27
		CCK (100 pM)	1.0 ± 0.50
		CCK (10 nM)	4.9 ± 0.87 *
	VAMP8-/-	Basal	1.1 ± 0.37
		CCK (100 pM)	0.8 ± 0.39
		Transfected Cells	
4 h	Wt GFP		1.3 ± 0.52
	Wt TeTx		1.0 ± 0.34
	VAMP8-/- GFP		1.2 ± 0.33
	VAMP8-/- TeTx		1.1 ± 0.19
16 h	Wt GFP		1.3 ± 0.17
	Wt D52		1.2 ± 0.47
	Wt TeTx		1.1 ± 0.31
	Wt D52 + TeTx		1.4 ± 0.32
	VAMP8-/- GFP		1.4 ± 0.21
	VAMP8-/- D52		1.3 ± 0.19

Acini Perifusion—Isolated acini were suspended in 1 ml of Bio-Gel P2 beads and perfused at a rate of 1 ml/min at 37 °C using a peristaltic pump as previously described (38, 39). Samples were collected each min over 20 min for amylase analysis.

Cellular Trypsin Activity—Total cellular trypsinogen was activated by incubation of lysates with enterokinase (1 ng/μl) for 1 h at 37 °C. Activated trypsin was measured fluorometrically as described previously (40, 41).

Tissue Fractionation—Post-nuclear supernatant, ZGs, cytosol, and microsomes were purified from mouse pancreas as described previously (36). Purification of ZGs from isolated acinar cells was conducted as described (37). Equal amounts of protein or DNA were separated by SDS-PAGE and analyzed by immunoblotting. Protein expression was quantified by densitometry.

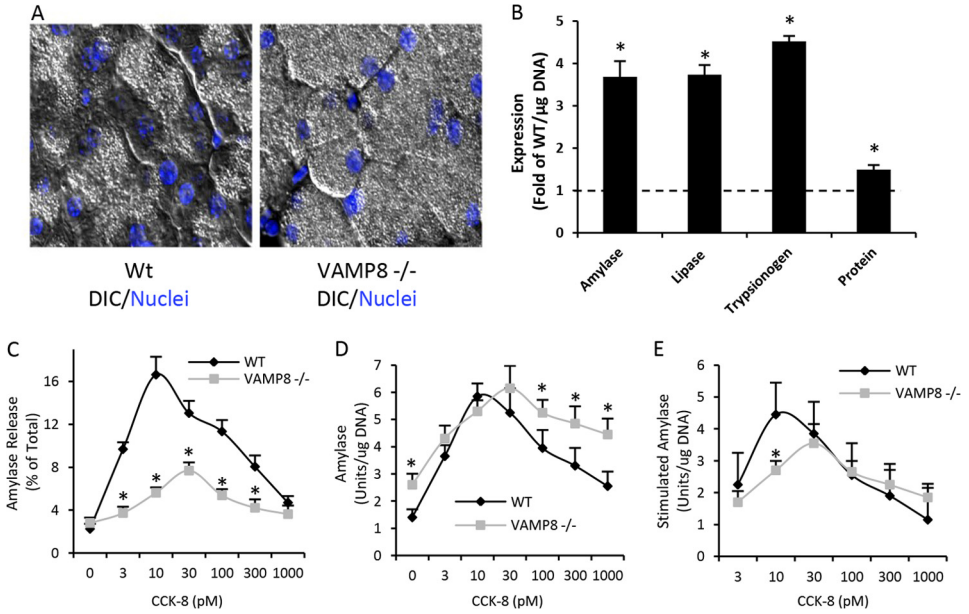

FIGURE 1. **VAMP8$^{-/-}$ acini secrete equivalent amounts of digestive enzymes as WT by enhancing constitutive secretion.** *A*, differential interference contrast (*DIC*) image of acini demonstrating a large accumulation of ZGs in VAMP8$^{-/-}$ *versus* WT cells. Nuclei are labeled in *blue*. *B*, amylase and trypsinogen enzyme activity, lipase immunoreactivity, and total cellular protein in WT *versus* VAMP8$^{-/-}$ acini normalized to total cellular DNA. WT levels are indicated by a *dashed line*. *C*, amylase secretion (30 min) from WT and VAMP8$^{-/-}$ acini stimulated with a range of CCK-8 concentrations and calculated as a percent of total cellular amylase. *D*, amylase activity secreted and normalized to cellular DNA. *E*, stimulated amylase release calculated by subtracting basal (WT = 1.4 ± 0.3%; VAMP8$^{-/-}$ = 2.6 ± 0.4%) from stimulated values. All data are the mean ± S.E. from at least three independent experiments, each performed in duplicate. *, $p <$ 0.05.

Fixation of Pancreatic Lobules and Immunofluorescence—Freshly prepared or cultured lobules were treated as indicated and fixed in 2% formaldehyde in 1× PBS for 2 h at room temp. After a series of sucrose dehydrations in 1× PBS at 4 °C, tissue was embedded in Tissue Tek and flash-frozen in liquid nitrogen-cooled isopentane. Antibody labeling of cryostat sections (8 μm) was from fresh or adenovirally infected lobules as previously described in detail (22).

Microscope Image Acquisition—Widefield images were captured using a Nikon Eclipse TE2000 microscope, a PlanApo ×100 oil objective with a numerical aperture of 1.4, and a Hamamatsu Orca camera. After collection, images were deconvolved and processed using Volocity software. Post collections, in some instances, pseudo colors were applied. Confocal images were captured using an inverted Nikon Eclipse Ti-E microscope, a Plan Apo × 100 oil objective with a numerical aperture of 1.4, a side-mounted scanhead, argon gas, DPSS and diode lasers, and a work station running NIS-Elements C software. Images were processed with Volocity or NIS-Elements AR software.

RESULTS

WT and VAMP8$^{-/-}$ Mice Undergo Equivalent Amounts of Amylase Secretion—VAMP8$^{-/-}$ mice reach normal weight at maturity and have a similar pancreatic weight as WT littermates (data not shown) but have a large accumulation of ZGs in acinar cells (8), which is easily identified by differential interference contrast microscopy (Fig. 1*A*). The accumulation in ZGs corresponds with increased amounts of total cell protein (1.5-fold) and the secretory digestive enzymes amylase (3.6-fold), lipase (3.7-fold), and trypsinogen (4.5-fold) when normalized to total cellular DNA (Fig. 1*A*).

Previous studies of VAMP8$^{-/-}$ pancreatic acini showed a significant reduction in carbachol- or CCK-induced amylase secretion when calculated as a percent of total cellular amylase (Fig. 1*C*) (8, 9). Because total cellular amylase is elevated nearly 4-fold in VAMP8$^{-/-}$ acini, we normalized secreted amylase activity to total cellular DNA revealing that VAMP8$^{-/-}$ acini in fact show equal amounts of secretion although they have a reduced sensitivity to CCK-8 with maximal effects seen at 30 pM CCK-8 *versus* 10 pM in WT (Fig. 1*D*). Interestingly, VAMP8$^{-/-}$ acini also show limited high dose secretory inhibition (<20% reduction from maximal stimulation compared with >50% reduction in WT acini). Subtraction of constitutive from total secretion demonstrated VAMP8$^{-/-}$ acini indeed have an ~45% reduction in maximally stimulated secretion but compensate by increased constitutive secretion (compare Fig. 1, *D* and *E*). Cytosolic lactate dehydrogenase release to the medium after 3 h of incubation of cells was extremely low (~1% of total cellular lactate dehydrogenase activity) confirming that the enhanced constitutive amylase secretion was not due to leakage from damaged cells (Table 1).

Elevated Constitutive Secretion in VAMP8$^{-/-}$ Acini Is Inhibited by cAMP—To eliminate the potential effects of VAMP8$^{-/-}$ on CCK receptor activation, cells were stimulated with thapsigargin (TG) to raise intracellular Ca^{2+}, phorbol ester (TPA) to mimic diacylglycerol, or CPT-cAMP (Fig. 2*A*). As seen in WT acini, TG, TPA, or their combination significantly increased secretion in VAMP8$^{-/-}$ acini with neither group showing an increase to CPT-cAMP alone. However, when added together with TG plus TPA (to mimic the effect of CCK-8), CPT-cAMP strongly potentiated secretion. Unexpectedly, analysis of stimulated secretion (constitutive subtracted from total) indicated

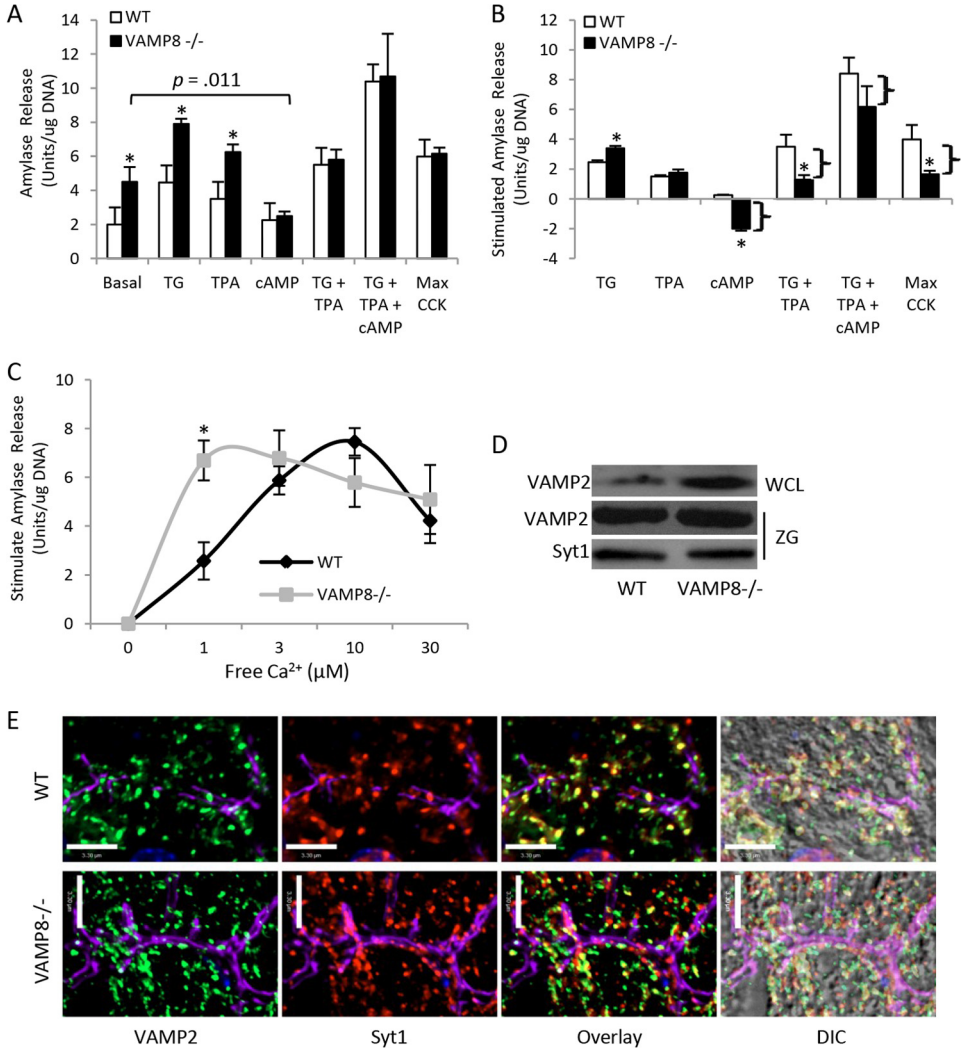

FIGURE 2. **Differential effects of cellular messengers on secretion in WT and VAMP8$^{-/-}$ acini.** *A*, amylase activity released from WT or VAMP8$^{-/-}$ acini treated with 2 μM TG, 1 μM TPA, 100 μM CPT-cAMP, or maximal (*Max*) CCK-8 (30 min) and normalized to cellular DNA. *B*, constitutive secretion (WT = 2.0 ± 0.3%; VAMP8$^{-/-}$ = 4.5 ± 0.9%) was subtracted from stimulated values in *A*. *C*, α-toxin permeabilized acini were stimulated with the indicated concentrations of Ca^{2+} for 30 min. Constitutive secretion (WT = 3.1 ± 1.1, VAMP8$^{-/-}$ = 8.1 ± 2.1) is subtracted and normalized to cellular DNA. All data are the mean ± S.E. from at least three independent experiments, each performed in duplicate. *, $p < 0.05$. *D*, immunoblotting of VAMP2 and syt1 in a whole cell lysate and purified ZG fractions from WT and VAMP8$^{-/-}$ acini (also see Fig. 5). *E*, widefield microscopy of 8-μm cryostat-sectioned pancreatic lobules from WT mice show punctate, compact apical colocalization of VAMP2 and syt1. VAMP8$^{-/-}$ acini show expanded punctate staining with moderately decreased colocalization. VAMP2 and syt1 immunoreactivities were detected using Alexa-Fluor 488-conjugated anti-mouse (1:100) and Alexa-Fluor 546-conjugated anti-rabbit (1:100), respectively. Actin localization was detected using phalloidin conjugated to Alexa-Fluor 694 (10 units/200 μl). Nuclei are stained with DAPI. *Scale bars*, 3.3 μm. Each image is a projection of reconstructed z-series images (~26 optical sections of 0.3 μm) and representative of multiple determinations from at least 3 separate tissue preparations. *DIC*, differential interference contrast.

CPT-cAMP significantly inhibited constitutive secretion in VAMP8$^{-/-}$ acini (Fig. 2*B*) with equivalent decreases also evident (*brackets* in VAMP8$^{-/-}$ acini) after the addition of TG plus TPA or maximal secretory concentrations of CCK-8. These data indicate that the high levels of constitutive secretion in VAMP8$^{-/-}$ acini are inhibited by cAMP; however, the ability of cAMP to potentiate secretion in response to Ca^{2+}/diacylglycerol remains intact.

Enhanced Ca^{2+} Sensitivity of Exocytosis in VAMP8$^{-/-}$ Acini—Although TPA-stimulated secretion was not altered in VAMP8$^{-/-}$ acini, a 35% increase in Ca^{2+}-stimulated secretion was detected. Secretagogue-stimulated Ca^{2+}-elevation was previously shown to be unaltered in VAMP8$^{-/-}$ acini (10). To further investigate the enhanced response to elevated Ca^{2+}, we permeabilized acinar cells with α-toxin to create small plasma membrane pores of ≤1 kDa molecular mass cut-off, thereby limiting the loss of cytoplasmic proteins. Clamping the Ca^{2+} concentration at various levels confirmed previous studies showing a biphasic secretory response with maximal secretion occurring at 10 μM Ca^{2+} and partial inhibition at higher concentrations (Fig. 2*C*) (42). VAMP8$^{-/-}$ acini demonstrated a 10-fold increased sensitivity with maximal secretion at 1 μM Ca^{2+} and, like WT, became inhibited at higher concentrations. We previously identified a potential role for the Ca^{2+}-sensing regulatory protein syt1 in VAMP2-mediated exocytosis (43). Analysis of VAMP2 in whole cell lysates revealed a 4-fold increase in VAMP8$^{-/-}$ acini consistent with the increased numbers of ZGs (Fig. 2*D*, also see Fig. 5). syt1 immunoreactivity is too low to detect in whole cell lysates. Alternatively, analysis of VAMP2 and syt1 in purified ZG fractions indicated equiva-

lent levels in WT and VAMP8$^{-/-}$, supporting that although the number of ZGs is greatly increased in VAMP8$^{-/-}$, the relative expression of VAMP2 and syt1 on these organelles remains constant. Immunofluorescence analysis confirmed the colocalization of VAMP2 and syt1 in WT and VAMP8$^{-/-}$ acini (Fig. 2*E*). These results support that the enhanced Ca^{2+} -sensitivity for secretion in VAMP$^{-/-}$ acini is a consequence of the large increase in VAMP2/syt1-positive ZGs.

VAMP2 ZGs Mediate an Early Rapid Phase and VAMP8 ZGs a Second Prolonged Phase of Secretion—We previously showed that VAMP2-positive ZGs are concentrated in the most apical aspects of the cytoplasm within cortical actin filaments and along the apical plasma membrane under basal conditions, whereas VAMP8 ZGs are recruited more slowly to the apical membrane after cell stimulation (6). Using a perifusion system to monitor secretion from a single group of cells over time demonstrates secretion initially peaks at 1 min and decreases over 2–3 min followed by a second prolonged phase that peaks and declines to near the initial constitutive levels over 20 min (Fig. 3*A*) (38, 39). In VAMP8$^{-/-}$ acini the initial rapid phase is slightly delayed by 1 min then quickly decays to constitutive levels by 3–5 min (see the *dotted line*) followed by a further decrease that approaches the constitutive levels seen in WT acini. Normalizing secretion to total cellular DNA (Fig. 3*B*) confirms VAMP8$^{-/-}$ has a higher constitutive secretion that produces almost equivalent amylase release over the full 20 min of stimulation (summated secretion is indicated at the end of each plot). Summation of amylase release from 5 to 20 min when secretion in VAMP8$^{-/-}$ falls below the initial constitutive levels indicates an ~45% decrease in VAMP8$^{-/-}$ *versus* WT acini over that period, in close agreement with the reduced secretory response seen for cAMP, TPA plus TG, or CCK-8 in VAMP8$^{-/-}$ acini (see the *brackets* in Fig. 2*B*). These results were consistent in multiple independent experiments (Fig. 3*C*).

VAMP2 and VAMP8 Are the Primary vSNAREs for Stimulated Secretion—VAMPs 2, 3, and 8 have been identified in pancreatic acinar cells with VAMP3 residing mainly in the Golgi and VAMP2 and VAMP8 present in both purified ZGs and the remaining microsomal fraction after ZG removal. The A-chain of TeTx specifically cleaves VAMP2 and -3 but not TeTx-insensitive (Ti)-VAMP7 or -VAMP8 (44, 45). The acute effects of VAMP2 cleavage in intact acinar cells were examined by short term (4 h) adenoviral expression of TeTx A-chain, which rapidly degrades >90% of VAMP2 (Fig. 4*A*). Acinar cells cultured for 4 h maintain a robust stimulated secretory response (see Fig. 6); however, maximal secretion was observed at 30 pM CCK-8 *versus* 10 pM in fresh acini. In agreement with previous studies conducted in permeabilized acini (4), VAMP2 cleavage in WT acini resulted in a 45% reduction in CCK-8 stimulated amylase (Fig. 4*D*) secretion compared with GFP expressing control acini but had no effect on constitutive secretion (Fig. 4*C*). In contrast, cleavage of VAMP2 in VAMP8$^{-/-}$ acini fully inhibited CCK-8-stimulated secretion. These data indicate that VAMP2 and -8 are the primary vSNAREs controlling secretagogue-stimulated ZG exocytosis and further identify an additional TeTx-resistant vSNARE that mediates constitutive secretion.

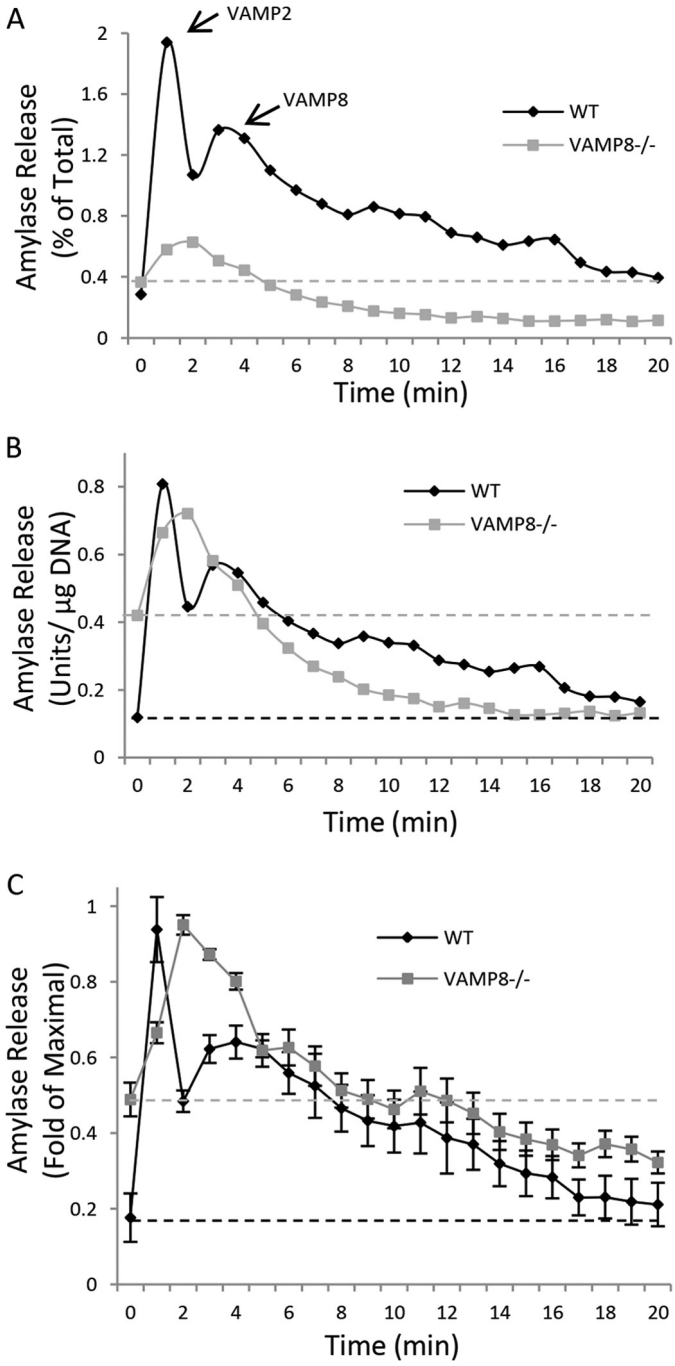

FIGURE 3. **VAMP2 mediates an early rapid- and VAMP8 a prolonged slow phase of acinar secretion.** Acini were embedded in Bio-Gel P-2 resin and perifused at 1 ml/min with maximal CCK-8 (WT = 10 pM, VAMP8$^{-/-}$ = 30 pM), and amylase released was analyzed each min for 20 min. *A*, a single representative experiment calculated as percent of total cellular amylase. Total summated secretion over the 20 min was 17.8 and 6.6% of total cellular amylase for WT and VAMP8$^{-/-}$, respectfully. *B*, the same experiment as in *panel A* normalized to cellular DNA (initial constitutive levels are indicated with *dashed lines*). Total summated secretion over 20 min was 7.4 and 7.6 units/μg of DNA for WT and VAMP8$^{-/-}$, respectfully. *C*, combined data (mean ± S.E.) from three independent experiments.

Loss of VAMP8 Alters Endosomal-regulatory Protein Expression and Subcellular Distribution—Analysis of protein expression normalized to cellular DNA confirmed that the ZG membrane and content proteins, VAMP2 and pancreatic lipase, respectively, were increased by 4-fold in VAMP8$^{-/-}$ acini (Fig.

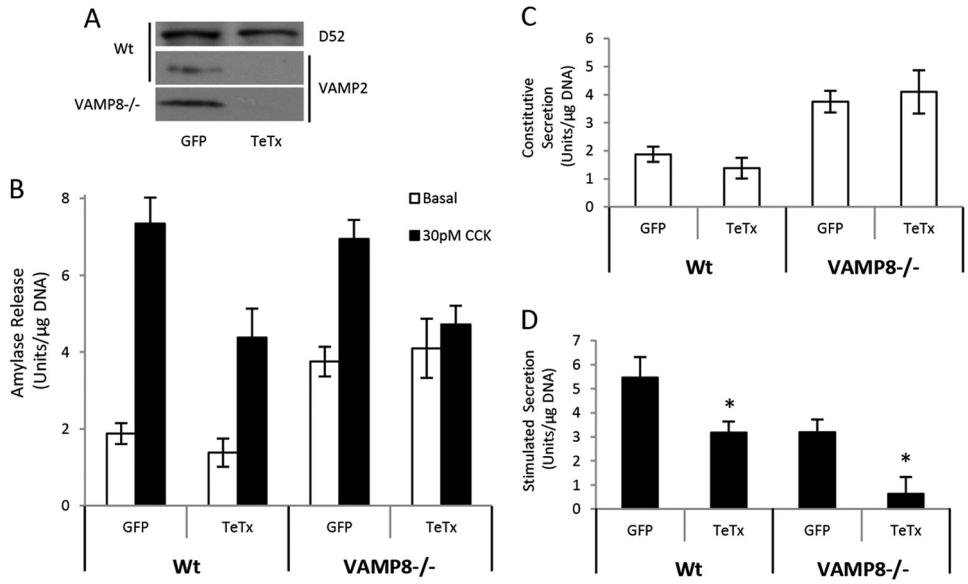

FIGURE 4. **VAMP2 and VAMP8 are the primary vSNAREs required for stimulated acinar secretion.** *A*, WT or VAMP8$^{-/-}$ acini were cultured for 4 h with adenovirus (4×10^6 pfu/ml) expressing GFP control or TeTx light chain. D52 and VAMP2 levels were analyzed by immunoblot. *B*, CCK-8-stimulated (30 pM) total amylase secretion from GFP or TeTx expressing acini (30 min). *C*, constitutive secretion replotted from *panel B*. *D*, stimulated secretion was calculated by subtracting constitutive from total secretion in *panel B*. Data are the mean ± S.E. from at least three independent experiments, each performed in duplicate. *, $p < 0.05$ compared with GFP control.

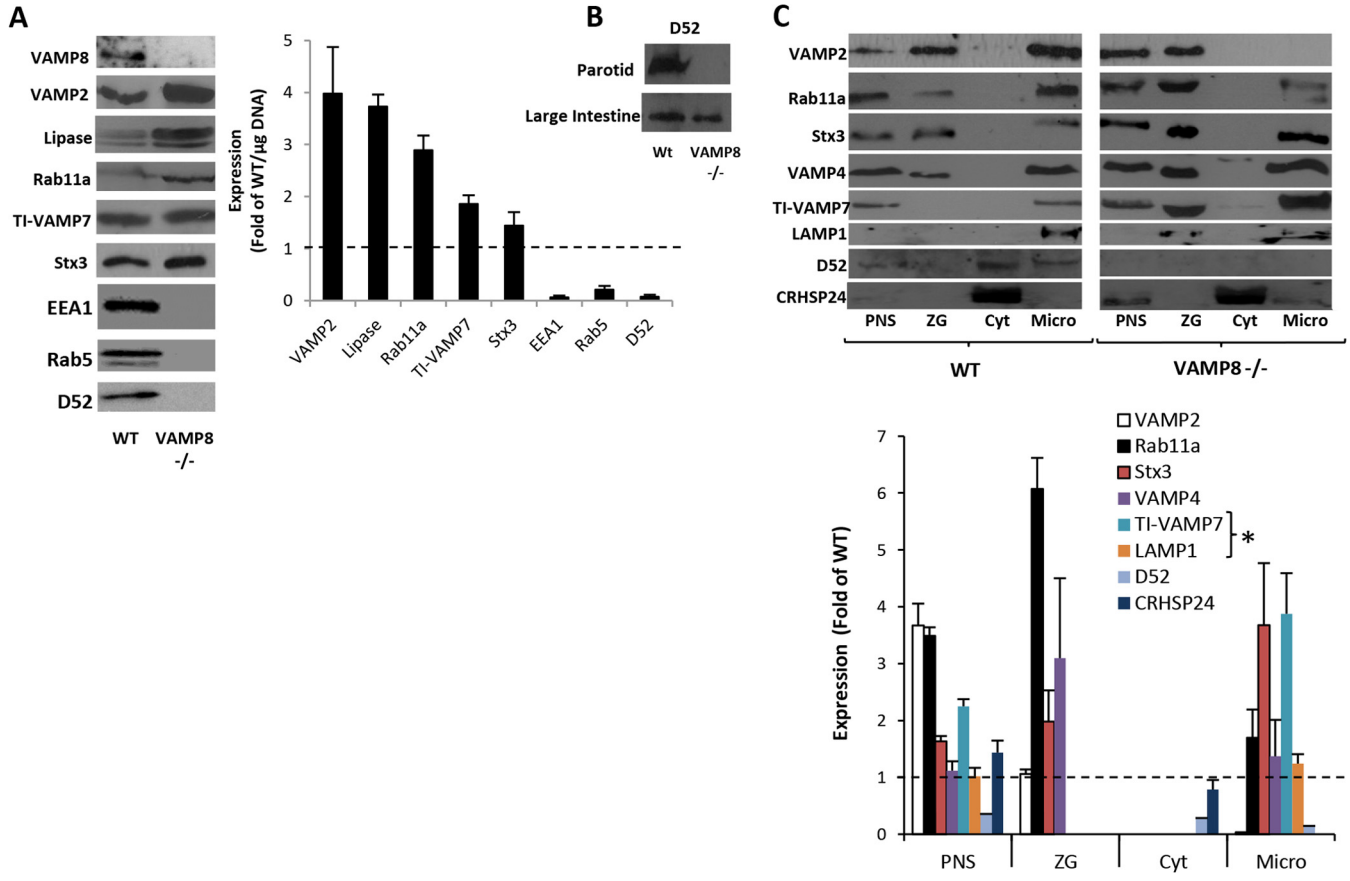

FIGURE 5. **Endosomal regulatory protein expression is greatly disrupted in VAMP8$^{-/-}$ acini.** *A*, equal amounts of DNA from WT or VAMP8$^{-/-}$ acini were loaded on SDS-PAGE gels, and the indicated proteins were analyzed by immunoblotting. Quantified expression is expressed as -fold WT (*dashed line*). *B*, immunoblot of D52 in homogenates from parotid gland and large intestine. *C*, subcellular fractionation of WT and VAMP8$^{-/-}$ pancreas was performed to obtain post nuclear supernatant (*PNS*), zymogen granule (*ZG*), cytosol (*Cyt*), and microsome (*Micro*) fractions. Equal amounts of protein from each fraction were immunoblotted with indicated antibodies. Quantified expression is indicated as -fold WT (*dashed line*). Data are the mean ± S.E. from at least three independent experiments except for VAMP4, which is the mean ± S.D. from two independent experiments. The *asterisk* indicates proteins that are not quantified in the ZG fractions due to their absence in Wt cells.

5*A*) (8). Interestingly, the RE protein Rab11a, which regulates apical endosomal trafficking in polarized epithelia, was elevated 3-fold (21, 46). Likewise, TI-VAMP7, which is thought to be the primary vSNARE for constitutive secretion in epithelia and neurons, was also elevated 2-fold in VAMP8$^{-/-}$ acini (47–49). The ZG and plasma membrane t-SNARE, syntaxin 3, was also slightly elevated. In contrast to ZG and RE proteins, the EE proteins EEA1, Rab5, and D52 were all reduced by >80% in VAMP8$^{-/-}$ acini compared with WT controls. Reduced levels of D52 were likewise observed in the parotid gland where VAMP8$^{-/-}$ acini show impaired secretion (Fig. 5*B*) (9). D52 levels were only slightly reduced in the large intestine where both VAMP8 and D52 are highly expressed in goblet cells, which represent a minor portion of the gland (32, 50).

Tissue fractionation and immunoblotting (normalized to total protein in each fraction) confirmed VAMP2 is present on ZGs and microsomes in WT pancreas and, although enriched in post nuclear supernatant, was unchanged in ZGs from VAMP8$^{-/-}$, indicating the level of VAMP2 per ZG remained constant (Fig. 5*C*). VAMP2 was absent in microsomes from VAMP8$^{-/-}$ pancreas potentially reflecting its large accumulation of ZGs. Rab11a, which is normally present in trace amounts on ZGs, was enhanced 7-fold in ZG fractions of VAMP8$^{-/-}$ pancreas, although this unusually large increase is likely reflected by the small denominator in the calculation. Similarly, the endosomal proteins TI-VAMP7 and LAMP1, which are normally absent from ZGs, were markedly enriched in ZGs from VAMP8$^{-/-}$ pancreas. Because of their absence from ZGs in WT acini, TI-VAMP7 and LAMP1 expression could not be expressed as a -fold change from WT in the accompanying graph. VAMP4, which is also TeTx-insensitive (51), was increased 3-fold in ZG fractions of VAMP8$^{-/-}$ acini but unchanged in post nuclear supernatant or microsomal fractions. Conversely, TI-VAMP7 was increased by 4-fold and Rab11a by 2-fold in microsomal fractions depleted of ZGs. Syntaxin 3, which is normally found on ZGs and microsomes, was also enriched in microsomal fractions from VAMP8$^{-/-}$ pancreas. D52, which is present in cytosol and microsomes, was greatly reduced in all VAMP8$^{-/-}$ fractions. The cytosolic protein, CRHSP24, was unchanged in WT and VAMP8$^{-/-}$ pancreas.

Immunofluorescence microscopy of VAMP2 and TI-VAMP7 indicated both molecules greatly expanded throughout the cytoplasm in VAMP8$^{-/-}$ acini (Fig. 6*A*). Close examination of apical cytoplasm indicated only minimal VAMP2/TI-VAMP7 colocalization present exclusively at the apical membrane in WT acini. In VAMP8$^{-/-}$ cells colocalization of TI-VAMP7 with VAMP2 or syt1 (not shown) was clearly evident on ZGs (Fig. 6*B*, *arrowheads*); however, both signals remained largely separate potentially, reflecting either separate ZG populations or, given the 4-fold increase in TI-VAMP7 in microsomal fractions (see Fig. 5*C*), post-Golgi/endosomal compartments. Consistent with previous studies (22, 52), Rab11a accumulates in the most apical regions of cytoplasm immediately beneath the actin filaments and plasma membrane (Fig. 6*C*, *arrows*). Additionally, some minor Rab11a immunoreactivity was present in supranuclear regions typically enriched in Golgi and post-Golgi derived endosomes (Fig. 6*C*, *arrowheads*). Unexpectedly,

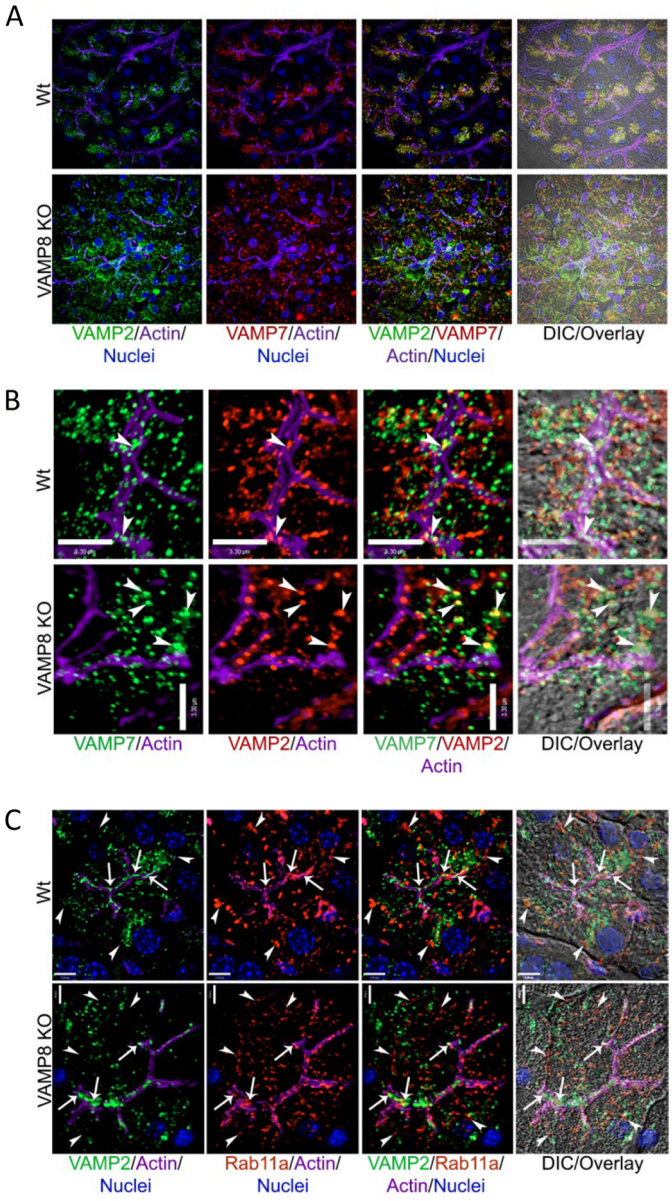

FIGURE 6. **VAMP2, Ti-VAMP7, and Rab11a show distinct localization patterns in WT *versus* VAMP8$^{-/-}$ acini.** Confocal (*A* and *C*) and widefield (*B*) microscopy of cryostat-sectioned pancreatic lobules from WT and VAMP8$^{-/-}$ mice. *A*, VAMP2 and VAMP7 immunoreactivities were detected with Alexa-Fluor 488-conjugated anti-chicken and Alexa-Fluor 546 conjugated anti-goat, respectively. *B*, VAMP2 and Ti-VAMP7 immunoreactivities were detected with Alexa-Fluor 546-conjugated anti-mouse and Alexa-Fluor 488-conjugated anti-goat, respectively. *Arrowheads* indicate punctate areas of colocalization. *C*, VAMP2 and Rab11a immunoreactivities were detected with Alexa-Fluor 488-conjugated anti-chicken and Alexa-Fluor 546-conjugated anti-rabbit, respectively. *Arrows* indicate the areas of colocalization of Rab11a with actin in the apical region. *Arrowheads* indicate punctate Rab11a labeling in perinuclear regions. Concentrations of all secondary antibodies were 1:100. Actin localization was detected using phalloidin conjugated to Alexa-Fluor 694 (10 units/200 μl). Nuclei are stained with DAPI. Confocal image *scale bars* are 5 μm. Widefield image *scale bars* are indicated. Each image is a projection of reconstructed z-series images (~26 optical sections of 0.3 μm) and representative of multiple determinations from at least 3 separate tissue preparations.

Rab11a showed only modest colocalization with Ti-VAMP7 even though both molecules were greatly expanded throughout the cytoplasm in VAMP8$^{-/-}$ acini (not shown). As we previously reported (22), minor colocalization of Rab11a and VAMP2 was seen in WT and VAMP8$^{-/-}$ acini confined mainly

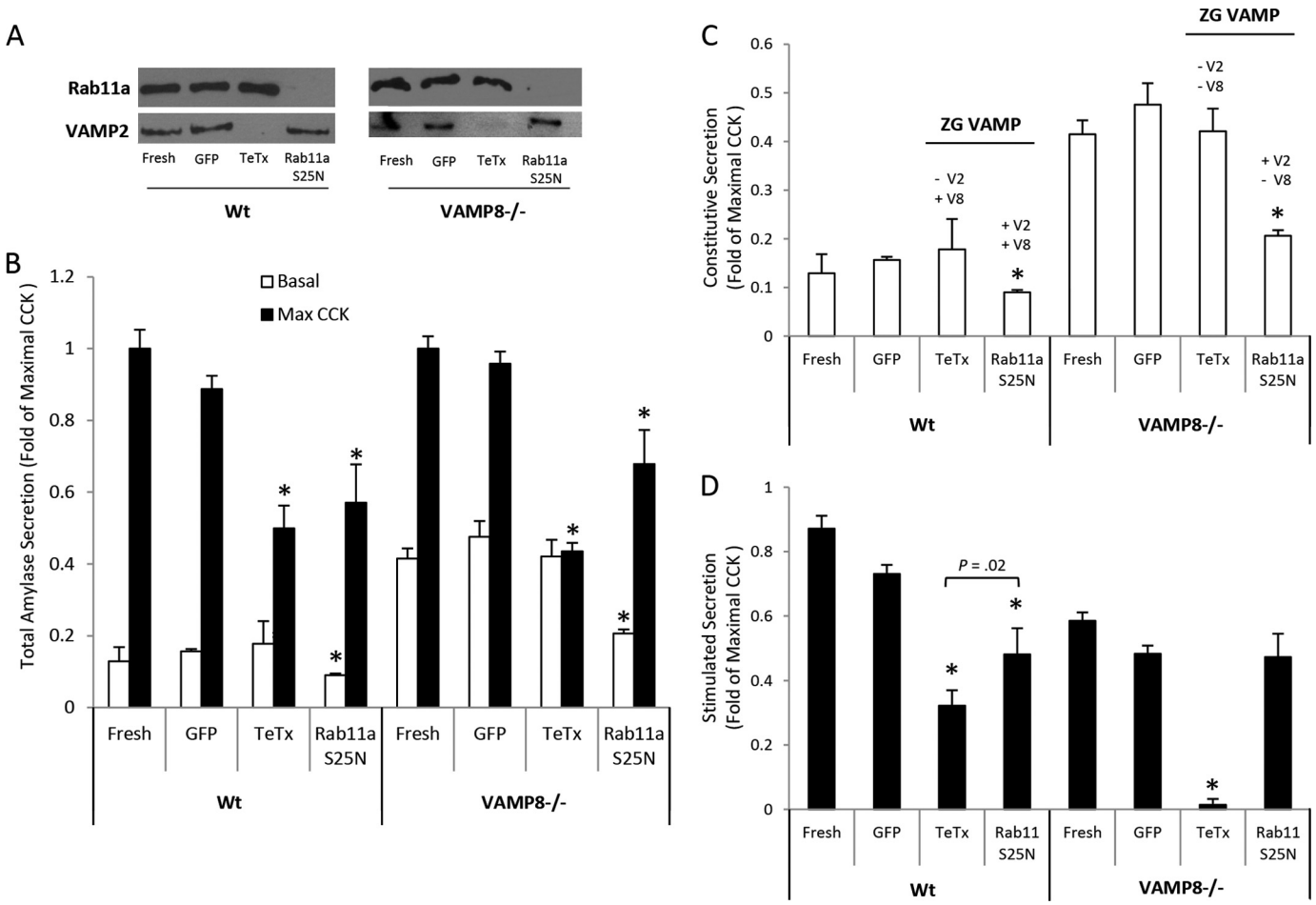

FIGURE 7. **Rab11a regulates VAMP8- but not VAMP2-mediated stimulated secretion.** VAMP8$^{-/-}$ acini were cultured for 6 h with GFP, TeTx, or EGFP-Rab11a (all at 1×10^6 pfu/ml) adenovirus. *A*, Rab11a and VAMP2 expression were analyzed by immunoblot. *B*, acini were left untreated or stimulated with 30 pM CCK-8 for 30 min. Stimulated secretion (*panel D*) was calculated by subtracting constitutive secretion (*panel C*) from total secretion. Data are the mean ± S.E. from at least three independent experiments each performed in duplicate. *, $p < 0.05$ compared with GFP control. Note acini cultured for 6 h show no reduction in secretion. ZG VAMP expression is indicated.

within the actin web and along the plasma membrane (Fig. 6*C*). Collectively, the limited colocalization of VAMP2-positive ZGs with Ti-VAMP7 and Rab11a likely underscores the dynamic nature of endosomal trafficking and its relationship to secretory granule maturation.

Rab11a Regulates Constitutive and Stimulated Secretion Independent of VAMP2—Because loss of VAMP8 increases ZG-associated Rab11a, we investigated how altering Rab11a activity would impact secretion. We have consistently seen in both rat and mouse acini that adenoviral expression of dominant negative (but not WT or constitutively active (not shown)) GDP-trapped Rab11a-S25N in either WT or VAMP8$^{-/-}$ acini results in a complete loss of endogenous Rab11a expression in 6 h (Fig. 7*A*). Moreover, 6-h cultured acini retain a robust secretory response when compared with freshly isolated cells (Fig. 7*B*). In WT acini, Rab11a-S25N significantly reduced both constitutive (Fig. 7*C*) and stimulated (Fig. 7*D*) secretion by ~40%. In VAMP8$^{-/-}$ acini, Rab11a-S25N reduced constitutive secretion by 50% but unlike WT had no effect on stimulated secretion. As shown in Fig. 4, TeTx cleavage of VAMP2 in VAMP8$^{-/-}$ acini had no effect on constitutive secretion and resulted in a complete loss of stimulated secretion. Collectively, these findings support that Rab11a acts on a VAMP8-containing secretory compartment to regulate stimulated secretion, whereas constitutive secretion is mediated by a TeTx-insensitive VAMP, presumably VAMP8 and/or TI-VAMP7.

The Endosomal System Is Essential for VAMP8-mediated Stimulated Secretion—We recently demonstrated that culturing rat acini for 16 h results in a loss of the EE protein Rab5 and its interacting proteins EEA1 and D52 together with a 50% decrease in stimulated secretion (22). Despite the reduced secretory response, the SNAREs (VAMPs 2 and 8 and syntaxins 2, 3, and 4) that regulate ZG exocytosis were unaltered. Moreover, adenoviral rescue of D52 coinduced Rab5 and EEA1 expression and restored the majority of the secretory phenotype, demonstrating an important role for the endosomal system in controlling acinar secretion. As seen in rat (22), a 14 h culture of WT mouse acini resulted in a 50% reduction in CCK-8-stimulated secretion and a >90% decrease in D52, Rab5, and EEA1 levels; however, VAMP2, TI-VAMP7, and Rab11a remained unchanged (Fig. 8, *A* and *B*). Interestingly, without culturing, freshly prepared VAMP8$^{-/-}$ acini, which normally contain low levels of these EE proteins, show an ~50% reduction in maximally stimulated secretion compared with WT (see Fig. 2*B*). Remarkably, VAMP8$^{-/-}$ acini show no decline in constitutive or stimulated secretion when cultured for 14 h, coin-

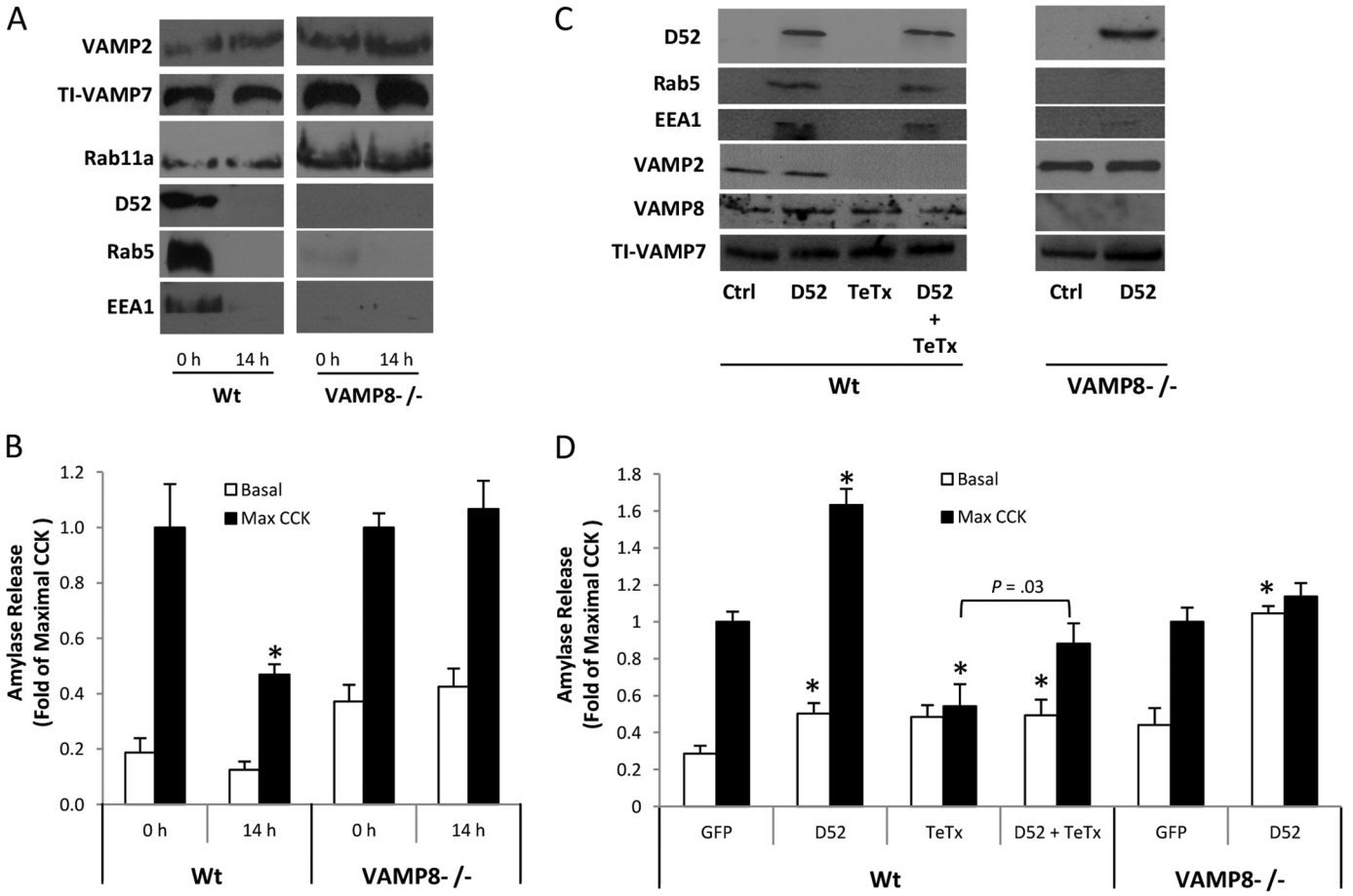

FIGURE 8. **Activation of the constitutive-like secretory pathway via D52/Rab5/EEA1 expression is required for VAMP8-mediated stimulated secretion.** *A* and *B*, WT or VAMP8$^{-/-}$ acini were cultured for 14 h, and expression of the indicated ZG and endosomal proteins was analyzed by immunoblot. Note the loss of D52, Rab5, and EEA1 in WT cultured cells and their absence in freshly prepared VAMP8$^{-/-}$ acini. Acini were either untreated or stimulated with maximal secretory concentrations of CCK-8 (fresh: WT = 10 pM, VAMP8$^{-/-}$ = 30 pM; cultured: WT and VAMP8$^{-/-}$ = 100 pM) for 30 min, and amylase secretion was determined. Note that VAMP8$^{-/-}$ shows no loss of secretory activity after culture. *C*, acini were cultured for 14 h with GFP (1×10^6), D52 (1×10^6), TeTx (1×10^6), or a combination (2×10^6 pfu/ml total), and the indicated ZG and endosomal proteins were analyzed by immunoblot. Note that D52 expression coinduces Rab5 and EEA1 in WT but not VAMP8$^{-/-}$ acini. *D*, WT or VAMP8$^{-/-}$ acini were cultured for 16 h with an adenovirus ($4 \times 10^{6.5}$ pfu/ml) expressing GFP control or D52 Wt. Acini were left untreated or stimulated with 100 pM CCK-8 for 30 min, and amylase secretion was measured. Note 1) that D52/Rab5/EEA1 expression restored TeTx-insensitive stimulated secretion in WT (*i.e.* the VAMP8 pathway), and 2) D52 expression in VAMP8$^{-/-}$ failed to coinduce Rab5 and EEA1 and markedly increased constitutive secretion. Data are the mean ± S.E. from at least three independent experiments, each performed in duplicate. *, $p < 0.05$ compared with GFP control.

cident with their low levels of endogenous endosomal proteins Rab5/EEA1/D52 (Fig. 8*B*). We, therefore, investigated the consequence of expressing D52 in WT *versus* VAMP8$^{-/-}$ acini. Identical to rat (22), D52 expression in mouse WT acini coinduced Rab5 and EEA1 expression and significantly enhanced both constitutive and stimulated secretion (Fig. 8, *C* and *D*). However, when expressed in VAMP8$^{-/-}$ acini, D52 failed to coinduce Rab5 and EEA1 yet markedly elevated constitutive secretion to stimulated levels preventing any further stimulated response. We next expressed TeTx to examine if loss of the EE regulatory proteins in WT acini after 14 h of culture would impact secretion from the VAMP2 secretory pathway. Strikingly, cleavage of VAMP2 fully inhibited stimulated secretion in cultured WT acini, indicating the VAMP8-mediated secretory pathway is lost together with the EE compartment. Moreover, when D52 expression was restored (together with coinduction of Rab5 and EEA1), TeTx cleavage of VAMP2 only partially inhibited stimulated secretion, indicating the VAMP8-mediated pathway was restored to 36% that of the total stimulated response; this level of restoration is highly significant as it represents 80% of VAMP8-mediated secretion in freshly prepared acini (see Figs. 3*D* and 6*D*).

Highly Expressed D52 Partially Localizes to ZGs—As we previously reported, D52 partially colocalizes with Rab11a in acini; however, unlike the trace amounts Rab11a present in purified ZGs, D52 is absent in these fractions (53). When more highly expressed in cultured pancreatic lobules, HA-tagged D52 extensively colocalizes with Rab11a (Fig. 9*A*). A similar pattern was detected for D52 and VAMP8 with the endogenous proteins discretely colocalizing in apical puncta, whereas with high expression of HA-D52, they show extensive colocalization (Fig. 9*B*). We recently reported that endogenous D52 and VAMP2 demonstrate little or no colocalization (22). In contrast to the pronounced D52/VAMP8 colocalization seen with HA-D52 expression, HA-D52 and VAMP2 showed much more limited colocalization. Fractionation of freshly prepared acini confirmed that D52 is absent in ZG fractions (Fig. 9*C*). Conversely, when expressed at high levels, significant HA-D52 immunore-

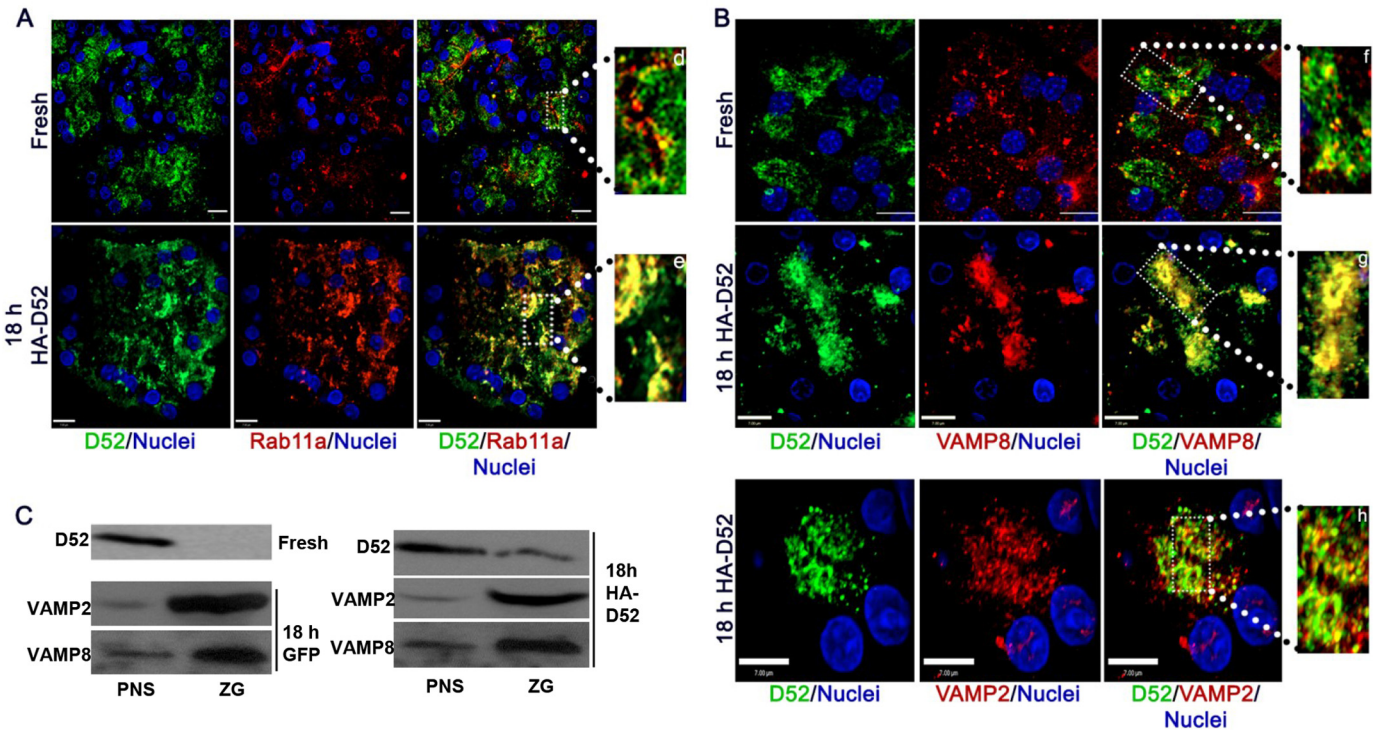

FIGURE 9. **Activation of the constitutive-like secretory pathway via D52/Rab5/EEA1 expression reveals strong colocalization of D52 with Rab11a and VAMP8.** Confocal (freshly prepared in *A* and *B*) or Brightfield (18 h culture expressing HA-D52 in *A* and *B*) microscopy of cryostat-sectioned lobules is shown. HA-D52 adenovirus was used at $10^{6.5}$ pfu/ml. *A*, D52 and Rab11a immunoreactivities were detected using Alexa-Fluor 546 conjugated anti-rabbit and Alexa-Fluor 488 conjugated anti-mouse respectively. *B*, D52 and VAMP8 immunoreactivities were detected in freshly prepared mouse lobules using Alexa-Fluor 546 conjugated anti-rabbit and Alexa-Fluor 488 conjugated anti-mouse. *Insets d* and *e* show magnified areas in the apical cytoplasm with distinct areas of punctate colocalization. For 18-h cultured rat lobules, HA-D52 (HA tag) and VAMP8 immunoreactivites were detected using Alexa-Fluor 546-conjugated anti-mouse and Alexa-Fluor 488-conjugated anti-rabbit. D52 and VAMP2 immunoreactivities were detected using Alexa-Fluor 546 conjugated anti-rabbit and Alexa-Fluor 488-conjugated anti-mouse. Pseudo colors were added post collection. Concentrations of all secondary antibodies were 1:100. Nuclei were stained with DAPI. Confocal image *scale bars* are 5 μm. Widefield image *scale bars* are as indicated. Each image is a projection from a reconstructed z-series images (~26 optical sections of 0.3 μm) and are representative of multiple determinations from at least 3 separate tissue preparations. *C*, ZGs were isolated from post nuclear supernatants (*PNS*) of fresh or 18 h cultured acini expressing HA-D52 and immunoblotted for indicated antibodies. Note the presence of highly expressed HA-D52 on ZGs.

activity was detected in ZG fractions, suggesting a direct communication between endosomal and ZG compartments. Taken together these findings support that endosomal trafficking plays a pivotal role in VAMP8-mediated ZG maturation and regulated exocytosis.

DISCUSSION

The current study demonstrates that VAMP8$^{-/-}$ in pancreatic acinar cells results in the enhanced expression and partial redistribution of TI-VAMP7, VAMP4, and Rab11a to ZGs and a compensatory increase in constitutive secretion. Expression of TeTx revealed that VAMP2 does not play a role in constitutive secretion, which is controlled by a TeTx-insensitive VAMP isoform of which VAMP4, -7, and -8 are candidates (51). In contrast, expression of the EE proteins Rab5, EEA1, and D52, which were recently shown to regulate endolysosome-like secretion via the CLP and MRP (22), were greatly reduced in VAMP8$^{-/-}$ acini. Characterization of the secretory response revealed that similar to nerve and endocrine cells, VAMP2-mediated exocytosis supports an early rapid phase of secretion, whereas the ubiquitously expressed VAMP8 is required for a second slower prolonged phase.

Unexpectedly the elevated constitutive secretion in VAMP8$^{-/-}$ acini was inhibited by elevation of cAMP with equivalent decreases also seen for thapsigargin plus TPA or maximal stimulatory levels of CCK-8. Furthermore, the pronounced decrease in constitutive secretion seen after CCK-8 stimulation in VAMP8$^{-/-}$ acini was identical to the inhibition seen with CPT-cAMP alone (compare Figs. 2 and 3). The mechanism(s) of cAMP signaling in pancreatic acinar secretion is still emerging. Evidence supports roles for both PKA and EPAC/Rap1 activation in stimulated secretion, the latter of which is also activated by CCK-8, Ca^{2+}, and diacylglycerol (54–56).

TeTx efficiently cleaves VAMP-1, -2 (synaptobrevins), and -3 (cellubrevin). Proteomic analysis of purified ZG membrane proteins showed only the presence of VAMP2 and VAMP8 but not VAMP1 or -3 (52). Furthermore, introduction of a soluble VAMP1 inhibitory construct into permeabilized acini failed to alter constitutive or stimulated secretion (6). A detailed study of VAMP3 immunoreactivity in acinar cells reported it is mainly present in Golgi and condensing vacuoles and is cleaved by the addition of TeTx to acinar lysates (57). It is, therefore, likely that VAMP3 was also acutely cleaved by TeTx in our studies (45). Results that constitutive secretion in both WT and VAMP8$^{-/-}$ acini is fully resistant to TeTx clearly support that it is not mediated by VAMP2 or -3. The extent of inhibition of stimulated secretion by short term TeTx expression is closely in line

with previous studies utilizing soluble VAMP2 inhibitory constructs (6) or neutralizing antibodies (7) and taken together with the lack of evidence for VAMP3 on ZGs strongly supports the secretory effects of TeTx in these studies were the result of VAMP2 cleavage.

Rab11a is normally found on a small subset of ZGs that localize to the very apical regions of cytoplasm but only minimally colocalize with VAMP2 (22, 52). Accordingly, minimal colocalization of Rab11a with VAMP2 was seen in VAMP8$^{-/-}$ acini despite its greatly expanded immunoreactivity. Although the trace levels of Rab11a normally detected on purified ZGs were increased 7-fold in VAMP8$^{-/-}$ cells, there was a 2-fold increase in microsomal fractions where Rab11a is most abundant in WT cells. Thus, the expanded immunoreactivity presumably represents an expansion of the RE compartment. Rab11a controls anterograde trafficking out of the EE and is the major regulator of RE generation, which in epithelial cells is essential to establish and maintain polarity (58). The large contraction of the Rab5/EEA1/D52 pathway in VAMP8$^{-/-}$ acini suggests either the small EE compartment was capable of supporting formation of the RE or that endocytic plasma membrane recycling was redirected directly to the RE or through the Golgi. Expression of GDP-trapped Rab11a-S25N inhibited constitutive secretion by 40–50% in both WT and VAMP8$^{-/-}$ acini but only inhibited stimulated secretion in the presence of VAMP8, indicating the redistribution of TI-VAMP7 and VAMP4 to ZGs in VAMP8$^{-/-}$ acini did not compensate for Rab11a-mediated stimulated secretion. More importantly, these results demonstrate that the effects of Rab11a on stimulated secretion are through the VAMP8 and not the VAMP2 secretory pathway.

Pancreatic acinar cells have an expanded EE compartment within the apical cytoplasm marked by high levels of Rab5, EEA1, and D52 (22, 53). The expanded endosomal compartment supports a large burden of plasma membrane retrieval after ZG exocytosis and also acts to recycle SNARE and accessory regulatory proteins necessary for ZG maturation and exocytosis. Interestingly, loss of VAMP8, which resides in EE and LE in most cells, results in a >80% decrease in Rab5, EEA1. and D52. Rab5 is proposed to be a master regulator of endosome biogenesis in cells as reduction of its expression to a critical threshold abolishes the entire endosomal system (59). Acini remain viable in VAMP8$^{-/-}$ mice, suggesting that although greatly reduced, Rab5 levels were sufficient to support endosomal and cellular function. In acini it appears VAMP8 may play a dual role in exocytosis and endocytic trafficking. During exocytosis VAMP8 can fuse with SNAP23 and syntaxin 4 present on the PM or with SNAP23 and syntaxin 3 present on ZGs for compound exocytosis (6). VAMP8 is also known to be active in the homotypic fusion of EEs and LEs as well as LE fusion with lysosomes (25, 60). A dual role for exocytotic SNAREs in endosomal fusion has been described for SNAP25 and VAMP2 in neuroendocrine and neuronal models (61, 62). Details regarding the endosomal itinerary of acinar SNARE proteins after their PM retrieval or how that pathway shapes ZG maturation are lacking.

Intriguingly, culturing WT acini for 14 h down-regulates Rab5, EEA1, and D52; however, VAMP8 levels on ZGs remain stable. Rescuing D52 expression coinduces Rab5 and EEA1, greatly enhances trafficking in the CLP, and restores much of the VAMP8 secretory response (see Fig. 8) (22). In contrast, in VAMP8$^{-/-}$ acini, which normally lack these proteins, D52 failed to coinduce Rab5 and EEA1 and greatly enhanced constitutive secretion. When expressed in CHO cells, D52 extensively colocalizes with TI-VAMP7 (63), which mediates the Ca^{2+}-dependent exocytosis of lysosome-like secretory organelles (64). Furthermore, high D52 expression in CHO cells causes a marked increase in constitutive lysosome-like secretion that is independent of elevated Ca^{2+} or D52 phosphorylation (63). Thus, it is conceivable that high D52 expression in the absence of VAMP8-ZGs results in high levels of post-Golgi Ti-VAMP7-mediated exocytosis as a consequence of the high Ti-VAMP7 expression. D52 was recently shown to interact with Rab5 (23), consistent with D52 localization to EE (53). Interestingly, expression of D52 strongly coinduces Rab5 and vice versa (not shown); however, the mechanism of coinduction and how it effects endosomal trafficking in the presence or absence of VAMP8 is unclear and currently under investigation.

We previously showed using LAMP1 external labeling that that expression of D52 in cultured acini enhanced anterograde endosomal trafficking via the CLP and caused a large accumulation of D52 in the Rab11a-positive RE compartment (22). LAMP1 labeling in the current study was precluded by its marked redistribution from microsomal to ZG fractions in VAMP8$^{-/-}$ acini. Here we also demonstrate that increasing EE trafficking in WT acini by high expression of D52 also causes a significant accumulation of D52 on VAMP8-positive ZGs that was detected by both ZG purification and immunofluorescence microscopy. D52 and VAMP8 colocalization is also apparent in freshly isolated WT acini; however, D52 does not copurify with ZGs. Conversely, low levels of Rab11a are detected in purified ZGs, and it too shows limited colocalization with both D52 (22) and ZGs (52) in freshly prepared WT pancreas (also see Fig. 9). It should be noted that unlike Rab11a, which is membrane-anchored by isoprenylation, D52 is a peripheral membrane protein abundant in cytosolic fractions. The appearance of D52 on purified ZGs seen when enhancing its expression may reflect a delay in its release to the cytosol after delivery from the endosomal compartment.

Similar to our findings, Azouz *et al.* (65), using high resolution live cell imaging, recently reported that Rab5-mediated trafficking from the EE controls the size and cargo composition of secretory granules in mast cells by a VAMP8-dependent fusion mechanism. We propose a similar mechanism where robust anterograde endosomal trafficking out of the EE via Rab11a is required for the maturation of VAMP8-positive ZGs. Results that 1) Rab11a specifically regulates the VAMP8 but not the VAMP2 pathway and 2) Rab11a is present on a small subset of ZGs as well as microsomal fractions suggest that it directs vesicle trafficking from the EE to both the ZG and RE compartments. One possibility is that upon cell stimulation trafficking within the Rab5/D52 and Rab11a pathways enhances VAMP8 ZG maturation thereby creating what was previously called the MRP. Thus a critical question that remains is whether the CLP/MRP have a dual function controlling ZG maturation and anterograde endosomal trafficking to the plasma membrane. In any case these results clearly underscore a pivotal role for the

endosomal system in shaping an optimal secretory response after ingestion of a meal when acinar cells remain highly active for a prolonged period.

REFERENCES

1. Palade, G. (1975) Intracellular aspects of the process of protein synthesis. *Science* **189,** 867
2. Jahn, R., and Scheller, R. H. (2006) SNAREs: engines for membrane fusion. *Nat. Rev. Mol. Cell Biol.* **7,** 631–643
3. Messenger, S. W., Falkowski, M. A., and Groblewski, G. E. (2014) Ca^{2+}-regulated secretory granule exocytosis in pancreatic and parotid acinar cells. *Cell Calcium* **55,** 369–375
4. Gaisano, H. Y., Sheu, L., Foskett, J. K., and Trimble, W. S. (1994) Tetanus toxin light chain cleaves a vesicle-associated membrane protein (VAMP) isoform 2 in rat pancreatic zymogen granules and inhibits enzyme secretion. *J. Biol. Chem.* **269,** 17062–17066
5. Fujita-Yoshigaki, J., Dohke, Y., Hara-Yokoyama, M., Kamata, Y., Kozaki, S., Furuyama, S., and Sugiya, H. (1996) Vesicle-associated membrane protein 2 is essential for cAMP-regulated exocytosis in rat parotid acinar cells. The inhibition of cAMP-dependent amylase release by botulinum neurotoxin B. *J. Biol. Chem.* **271,** 13130–13134
6. Weng, N., Thomas, D. D., and Groblewski, G. E. (2007) Pancreatic acinar cells express vesicle-associated membrane protein 2- and 8-specific populations of zymogen granules with distinct and overlapping roles in secretion. *J. Biol. Chem.* **282,** 9635–9645
7. Pickett, J. A., Campos-Toimil, M., Thomas, P., and Edwardson, J. M. (2007) Identification of SNAREs that mediate zymogen granule exocytosis. *Biochem. Biophys. Res. Commun.* **359,** 599–603
8. Wang, C.-C., Ng, C. P., Lu, L., Atlashkin, V., Zhang, W., Seet, L.-F., and Hong, W. (2004) A role of VAMP8/endobrevin in regulated exocytosis of pancreatic acinar cells. *Dev. Cell* **7,** 359–371
9. Wang, C.-C., Shi, H., Guo, K., Ng, C. P., Li, J., Gan, B. Q., Chien Liew, H., Leinonen, J., Rajaniemi, H., Zhou, Z. H., Zeng, Q., and Hong, W. (2007) VAMP8/endobrevin as a general vesicular SNARE for regulated exocytosis of the exocrine system. *Mol. Biol. Cell* **18,** 1056–1063
10. Cosen-Binker, L. I., Binker, M. G., Wang, C.-C., Hong, W., and Gaisano, H. Y. (2008) VAMP8 is the v-SNARE that mediates basolateral exocytosis in a mouse model of alcoholic pancreatitis. *J. Clin. Invest.* **118,** 2535–2551
11. Thorn, P., and Gaisano, H. (2012) Molecular control of compound exocytosis: a key role for VAMP8. *Commun. Integr. Biol.* **5,** 61–63
12. Gaisano, H. Y., and Gorelick, F. S. (2009) New insights into the mechanisms of pancreatitis. *Gastroenterology* **136,** 2040–2044
13. Nemoto, T., Kimura, R., Ito, K., Tachikawa, A., Miyashita, Y., Iino, M., and Kasai, H. (2001) Sequential-replenishment mechanism of exocytosis in pancreatic acini. *Nat. Cell Biol.* **3,** 253–258
14. Chen, Y., Warner, J. D., Yule, D. I., and Giovannucci, D. R. (2005) Spatiotemporal analysis of exocytosis in mouse parotid acinar cells. *Am. J. Physiol. Cell Physiol.* **289,** C1209–C1219
15. Behrendorff, N., Dolai, S., Hong, W., Gaisano, H. Y., and Thorn, P. (2011) Vesicle-associated membrane protein 8 (VAMP8) is a SNARE (soluble *N*-ethylmaleimide-sensitive factor attachment protein receptor) selectively required for sequential granule-to-granule fusion. *J. Biol. Chem.* **286,** 29627–29634
16. Masedunskas, A., and Weigert, R. (2008) Intravital two-photon microscopy for studying the uptake and trafficking of fluorescently conjugated molecules in live rodents. *Traffic* **9,** 1801–1810
17. Arvan, P., Kuliawat, R., Prabakaran, D., Zavacki, A. M., Elahi, D., Wang, S., and Pilkey, D. (1991) Protein discharge from immature secretory granules displays both regulated and constitutive characteristics. *J. Biol. Chem.* **266,** 14171–14174
18. Castle, J. D., and Castle, A. M. (1996) Two regulated secretory pathways for newly synthesized parotid salivary proteins are distinguished by doses of secretagogues. *J. Cell Sci.* **109,** 2591–2599
19. Huang, A. Y., Castle, A. M., Hinton, B. T., and Castle, J. D. (2001) Resting (basal) secretion of proteins is provided by the minor regulated and constitutive-like pathways and not granule exocytosis in parotid acinar cells. *J. Biol. Chem.* **276,** 22296–22306
20. Arvan, P., and Castle, D. (1998) Sorting and storage during secretory granule biogenesis: looking backward and looking forward. *Biochem. J.* **332,** 593–610
21. Castle, A. M., Huang, A. Y., and Castle, J. D. (2002) The minor regulated pathway, a rapid component of salivary secretion, may provide docking/fusion sites for granule exocytosis at the apical surface of acinar cells. *J. Cell Sci.* **115,** 2963–2973
22. Messenger, S. W., Thomas, D. D., Falkowski, M. A., Byrne, J. A., Gorelick, F. S., and Groblewski, G. E. (2013) Tumor protein D52 controls trafficking of an apical endolysosomal secretory pathway in pancreatic acinar cells. *Am. J. Physiol. Gastrointest. Liver Physiol.* **305,** G439–G452
23. Shahheydari, H., Frost, S., Smith, B. J., Groblewski, G. E., Chen, Y., and Byrne, J. A. (2014) Identification of PLP2 and RAB5C as novel TPD52 binding partners through yeast two-hybrid screening. *Mol. Biol. Rep.* **41,** 4565–4572
24. Christoforidis, S., McBride, H. M., Burgoyne, R. D., and Zerial, M. (1999) The Rab5 effector EEA1 is a core component of endosome docking. *Nature* **397,** 621–625
25. Antonin, W., Holroyd, C., Tikkanen, R., Höning, S., and Jahn, R. (2000) The R-SNARE endobrevin/VAMP-8 mediates homotypic fusion of early endosomes and late endosomes. *Mol. Biol. Cell* **11,** 3289–3298
26. Loo, L. S., Hwang, L.-A., Ong, Y. M., Tay, H. S., Wang, C.-C., and Hong, W. (2009) A role for endobrevin/VAMP8 in CTL lytic granule exocytosis. *Eur. J. Immunol.* **39,** 3520–3528
27. Paumet, F., Le Mao, J., Martin, S., Galli, T., David, B., Blank, U., and Roa, M. (2000) Soluble NSF attachment protein receptors (SNAREs) in RBL-2H3 mast cells: functional role of syntaxin 4 in exocytosis and identification of a vesicle-associated membrane protein 8-containing secretory compartment. *J. Immunol.* **164,** 5850–5857
28. Polgár, J., Chung, S.-H., and Reed, G. L. (2002) Vesicle-associated membrane protein 3 (VAMP-3) and VAMP-8 are present in human platelets and are required for granule secretion. *Blood* **100,** 1081–1083
29. Jones, L. C., Moussa, L., Fulcher, M. L., Zhu, Y., Hudson, E. J., O'Neal, W. K., Randell, S. H., Lazarowski, E. R., Boucher, R. C., and Kreda, S. M. (2012) VAMP8 is a vesicle SNARE that regulates mucin secretion in airway goblet cells. *J. Physiol.* **590,** 545–562
30. Zhu, D., Zhang, Y., Lam, P. P., Dolai, S., Liu, Y., Cai, E. P., Choi, D., Schroer, S. A., Kang, Y., Allister, E. M., Qin, T., Wheeler, M. B., Wang, C.-C., Hong, W.-J., Woo, M., and Gaisano, H. Y. (2012) Dual role of VAMP8 in regulating insulin exocytosis and islet β cell growth. *Cell Metab.* **16,** 238–249
31. Südhof, T. C. (2013) Neurotransmitter release: the last millisecond in the life of a synaptic vesicle. *Neuron* **80,** 675–690
32. Groblewski, G. E., Yoshida, M., Yao, H., Williams, J. A., and Ernst, S. A. (1999) Immunolocalization of CRHSP28 in exocrine digestive glands and gastrointestinal tissues of the rat. *Am. J. Physiol.* **276,** G219–G226
33. Groblewski, G. E., Yoshida, M., Bragado, M. J., Ernst, S. A., Leykam, J., and Williams, J. A. (1998) Purification and characterization of a novel physiological substrate for calcineurin in mammalian cells. *J. Biol. Chem.* **273,** 22738–22744
34. Lowe, M. E. (1992) The catalytic site residues and interfacial binding of human pancreatic lipase. *J. Biol. Chem.* **267,** 17069–17073
35. Teng, Q., Tanase, D., Tanase, D. K., Liu, J. K., Garrity-Moses, M. E., Baker, K. B., and Boulis, N. M. (2005) Adenoviral clostridial light chain gene-based synaptic inhibition through neuronal synaptobrevin elimination. *Gene. Ther.* **12,** 108–119
36. Thomas, D. D., Taft, W. B., Kaspar, K. M., and Groblewski, G. E. (2001) CRHSP-28 regulates Ca^{2+}-stimulated secretion in permeabilized acinar cells. *J. Biol. Chem.* **276,** 28866–28872
37. Chen, X., Ernst, S. A., and Williams, J. A. (2003) Dominant negative Rab3D mutants reduce GTP-bound endogenous Rab3D in pancreatic acini. *J. Biol. Chem.* **278,** 50053–50060
38. Yoshimura, K., and Nezu, E. (1991) Dynamic changes in the rate of amylase release induced by various secretagogues examined in isolated rat parotid cells by using column perifusion. *Jpn. J. Physiol.* **41,** 443–459
39. Yoshimura, K., and Hiramatsu, Y. (1998) Characteristics of amylase secretion induced by various secretagogues examined in perifused rat parotid acinar cells. *Eur. J. Morphol.* **36,** 198–202
40. Baumler, M. D., Koopmann, M. C., Thomas, D. D., Ney, D. M., and Gro-

blewski, G. E. (2010) Intravenous or luminal amino acids are insufficient to maintain pancreatic growth and digestive enzyme expression in the absence of intact dietary protein. *Am. J. Physiol. Gastrointest. Liver Physiol.* **299,** G338–G347
41. Kawabata, S., Miura, T., Morita, T., Kato, H., Fujikawa, K., Iwanaga, S., Takada, K., Kimura, T., and Sakakibara, S. (1988) Highly sensitive peptide-4-methylcoumaryl-7-amide substrates for blood-clotting proteases and trypsin. *Eur. J. Biochem.* **172,** 17–25
42. Padfield, P. J., and Panesar, N. (1995) Ca^{2+}-dependent amylase secretion from SLO-permeabilized rat pancreatic acini requires diffusible cytosolic proteins. *Am. J. Physiol.* **269,** G647–G652
43. Falkowski, M. A., Thomas, D. D., Messenger, S. W., Martin, T. F., and Groblewski, G. E. (2011) Expression, localization, and functional role for synaptotagmins in pancreatic acinar cells. *Am. J. Physiol. Gastrointest. Liver Physiol.* **301,** G306–G316
44. Schiavo, G., Benfenati, F., Poulain, B., Rossetto, O., Polverino de Laureto, P., DasGupta, B. R., and Montecucco, C. (1992) Tetanus and botulinum-B neurotoxins block neurotransmitter release by proteolytic cleavage of synaptobrevin. *Nature* **359,** 832–835
45. McMahon, H. T., Ushkaryov, Y. A., Edelmann, L., Link, E., Binz, T., Niemann, H., Jahn, R., and Südhof, T. C. (1993) Cellubrevin is a ubiquitous tetanus-toxin substrate homologous to a putative synaptic vesicle fusion protein. *Nature* **364,** 346–349
46. Baetz, N. W., and Goldenring, J. R. (2013) Rab11-family interacting proteins define spatially and temporally distinct regions within the dynamic Rab11a-dependent recycling system. *Mol. Biol. Cell* **24,** 643–658
47. Pocard, T., Le Bivic, A., Galli, T., and Zurzolo, C. (2007) Distinct v-SNAREs regulate direct and indirect apical delivery in polarized epithelial cells. *J. Cell Sci.* **120,** 3309–3320
48. Oishi, Y., Arakawa, T., Tanimura, A., Itakura, M., Takahashi, M., Tajima, Y., Mizoguchi, I., and Takuma, T. (2006) Role of VAMP-2, VAMP-7, and VAMP-8 in constitutive exocytosis from HSY cells. *Histochem. Cell Biol.* **125,** 273–281
49. Scheuber, A., Rudge, R., Danglot, L., Raposo, G., Binz, T., Poncer, J.-C., and Galli, T. (2006) Loss of AP-3 function affects spontaneous and evoked release at hippocampal mossy fiber synapses. *Proc. Natl. Acad. Sci. U.S.A.* **103,** 16562–16567
50. Rodríguez-Piñeiro, A. M., van der Post, S., Johansson, M. E., Thomsson, K. A., Nesvizhskii, A. I., and Hansson, G. C. (2012) Proteomic study of the mucin granulae in an intestinal goblet cell model. *J. Proteome Res.* **11,** 1879–1890
51. Mallard, F., Tang, B. L., Galli, T., Tenza, D., Saint-Pol, A., Yue, X., Antony, C., Hong, W., Goud, B., and Johannes, L. (2002) Early/recycling endosomes-to-TGN transport involves two SNARE complexes and a Rab6 isoform. *J. Cell Biol.* **156,** 653–664
52. Chen, X., Ulintz, P. J., Simon, E. S., Williams, J. A., and Andrews, P. C. (2008) Global topology analysis of pancreatic zymogen granule membrane proteins. *Mol. Cell Proteomics* **7,** 2323–2336
53. Thomas, D. D., Weng, N., and Groblewski, G. E. (2004) Secretagogue-induced translocation of CRHSP-28 within an early apical endosomal compartment in acinar cells. *Am. J. Physiol. Gastrointest. Liver Physiol.* **287,** G253–G263
54. Williams, J. A. (2008) Receptor-mediated signal transduction pathways and the regulation of pancreatic acinar cell function. *Curr. Opin. Gastroenterol.* **24,** 573–579
55. Sabbatini, M. E., Chen, X., Ernst, S. A., and Williams, J. A. (2008) Rap1 activation plays a regulatory role in pancreatic amylase secretion. *J. Biol. Chem.* **283,** 23884–23894
56. Chaudhuri, A., Husain, S. Z., Kolodecik, T. R., Grant, W. M., and Gorelick, F. S. (2007) Cyclic AMP-dependent protein kinase and Epac mediate cyclic AMP responses in pancreatic acini. *Am. J. Physiol. Gastrointest. Liver Physiol.* **292,** G1403–G1410
57. Sengupta, D., Gumkowski, F. D., Tang, L. H., Chilcote, T. J., and Jamieson, J. D. (1996) Localization of cellubrevin to the Golgi complex in pancreatic acinar cells. *Eur. J. Cell Biol.* **70,** 306–314
58. Hoekstra, D., Tyteca, D., and van IJzendoorn, S. C. (2004) The subapical compartment: a traffic center in membrane polarity development. *J. Cell Sci.* **117,** 2183–2192
59. Zeigerer, A., Gilleron, J., Bogorad, R. L., Marsico, G., Nonaka, H., Seifert, S., Epstein-Barash, H., Kuchimanchi, S., Peng, C. G., Ruda, V. M., Del Conte-Zerial, P., Hengstler, J. G., Kalaidzidis, Y., Koteliansky, V., and Zerial, M. (2012) Rab5 is necessary for the biogenesis of the endolysosomal system *in vivo*. *Nature* **485,** 465–470
60. Mullock, B. M., Smith, C. W., Ihrke, G., Bright, N. A., Lindsay, M., Parkinson, E. J., Brooks, D. A., Parton, R. G., James, D. E., Luzio, J. P., and Piper, R. C. (2000) Syntaxin 7 is localized to late endosome compartments, associates with Vamp 8, and Is required for late endosome-lysosome fusion. *Mol. Biol. Cell* **11,** 3137–3153
61. Aikawa, Y., Lynch, K. L., Boswell, K. L., and Martin, T. F. (2006) A second SNARE role for exocytic SNAP25 in endosome fusion. *Mol. Biol. Cell* **17,** 2113–2124
62. Zhang, Z., Wang, D., Sun, T., Xu, J., Chiang, H.-C., Shin, W., and Wu, L.-G. (2013) The SNARE proteins SNAP25 and synaptobrevin are involved in endocytosis at hippocampal synapses. *J. Neurosci.* **33,** 9169–9175
63. Thomas, D. D., Martin, C. L., Weng, N., Byrne, J. A., and Groblewski, G. E. (2010) Tumor protein D52 expression and Ca^{2+}-dependent phosphorylation modulates lysosomal membrane protein trafficking to the plasma membrane. *Am. J. Physiol. Cell Physiol.* **298,** C725–C739
64. Rao, S. K., Huynh, C., Proux-Gillardeaux, V., Galli, T., and Andrews, N. W. (2004) Identification of SNAREs involved in synaptotagmin VII-regulated lysosomal exocytosis. *J. Biol. Chem.* **279,** 20471–20479
65. Azouz, N. P., Zur, N., Efergan, A., Ohbayashi, N., Fukuda, M., Amihai, D., Hammel, I., Rothenberg, M. E., and Sagi-Eisenberg, R. (2014) Rab5 is a novel regulator of mast cell secretory granules: impact on size, cargo, and exocytosis. *J. Immunol.* **192,** 4043–4053